

## *Supporting Information*

# Donor-acceptor covalent organic framework promotes visible light-induced oxidative coupling of amines to imines in air

Jingwen Feng <sup>#</sup>, Jie Cheng <sup>#</sup>, Jun Pang, Mingqiang Tang, Zewei Liu, Chunying Rong, and Rong

Tan\*

National & Local Joint Engineering Laboratory for New Petro-chemical Materials and Fine Utilization of Resources; Key Laboratory of Chemical Biology and Traditional Chinese Medicine Research (Ministry of Education); Key Laboratory of the Assembly and Application of Organic Functional Molecules of Hunan Province, College of Chemistry & Chemical Engineering, Hunan Normal University, No.36, South Lushan Road, Changsha, Hunan 410081 (P. R. China).

\*Corresponding author. Email: yiyangtanrong@126.com.

<sup>#</sup> These authors should be considered as co-first authors since they contributed equally to this work.

Number of pages: 6 (from S1 to S10)

Number of figures: 8

**CONTENT:**

1. Nitrogen adsorption-desorption of the obtained COFs
2. Apparent quantum efficiency (AQE) for the formation of *N*-benzylidenebenzylamine over

**TpTt-COF**

3. <sup>1</sup>H NMR spectra of the obtained condensation products

## 1. Nitrogen adsorption-desorption of the obtained COFs

Nitrogen adsorption-desorption was used to analyze the porosity of the obtained COFs, as shown in Figure S1. Both **TpTt-COF** and **TfTa-COF** showed a combined type-I/IV isotherm with type H3 hysteresis loop (Figure S1-A), which suggests the coexistence of micropores and mesopores in the hybrid materials [1]. The hierarchical porous structure is authenticated by the corresponding pore size distribution. Clearly, they show the micropores at around 1.41 nm, as well as a continuous pore diameter distribution in the range greater than 4.0 nm (Figure S1-B). We deduce that the micropore of 1.41 nm should originate from the inherent pores of **TpTt-COF** and **TfTa-COF**, while the mesopores with the size greater than 4.0 nm may be arise from the layer stacking of 2D COF sheets. The high porosity should increase the accessibility of active sites, and especially, enable rapid diffusion of charges to surface, which are desirable for the visible light-driven chemical transformation.

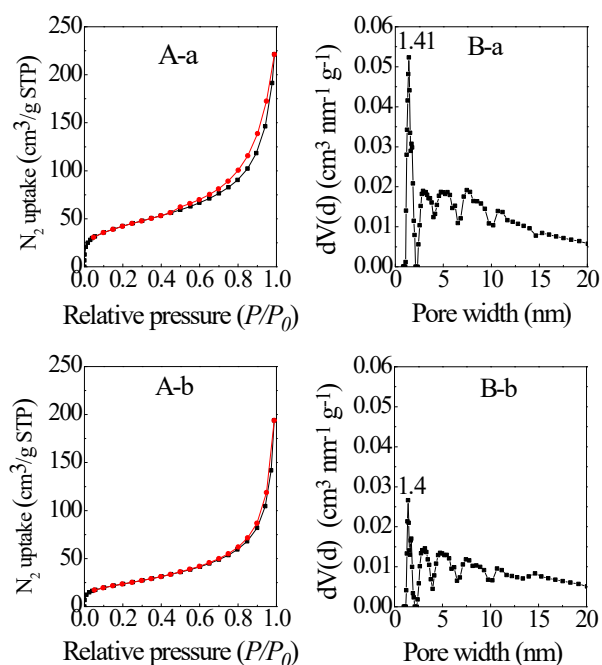


**Figure S1.** Nitrogen adsorption-desorption isotherm (A) and the corresponding pore size distribution plots (B) of **TpTt-COF** (a) and **TfTa-COF** (b)

2. Apparent quantum efficiency (AQE) for the formation of *N*-benzylidenebenzylamine over **TpTt-COF**

A commercial photo-reactor using xenon lamp as an external illumination was used to examine the apparent quantum efficiency (AQE). Monochromatic visible light at 450 nm was obtained by attaching bandpass filters to the xenon lamp and used as an external illumination. After external illumination for 30 min with xenon lamp (300 W lamp power), 47% yield of *N*-benzylidenebenzylamine selectivity over **TpTt-COF** were obtained on this photo-reactor. The AQE value was calculated using the equation [2]:

$$AQE = \frac{n \times M \times N_A \times h \times c}{S \times P \times t \times \lambda} \times 100\%$$

Where *n* is the number of reaction electron (2 for benzylamine oxidation); *M* is the molar amounts of *N*-benzylidenebenzylamine formed ( $9.4 \times 10^{-5}$  mol);  $N_A$  is the avogadro constant ( $6.022 \times 10^{23}$ ); *h* is the Planck constant ( $6.626 \times 10^{-34}$  J·s); *c* is the speed of light ( $3.0 \times 10^8$  m/s); *S* is the irradiation area (6.25 cm<sup>2</sup>); *P* is the incident light intensity at certain wavelength ( $3.4 \times 10^{-2}$  W·cm<sup>-2</sup>); *t* is the irradiation time (1800 s);  $\lambda$  is the monochromatic light wavelength (450 nm).

Therefore, the AQE for the formation of *N*-benzylidenebenzylamine over **TpTt-COF** was calculated to be *ca.* 13.1%. It outperformed other photocatalysts previously studied under similar experimental conditions, whose AQY was reported to be less than 11%, as shown in Table S1.

**Table S1.** Comparisons of AQE values of different catalysts for benzylamine oxidation under

visible light irradiation				
Entry	Catalyst	Wavelength of incident light (nm)	AQY value (%)	Reference

1	<b>TpTt-COF</b>	450	13.1	in this work
2	HNb <sub>3</sub> O <sub>8</sub> NS U	420	6.57	[3]
3	Nb <sub>2</sub> O <sub>5</sub> NR	420	0.82	[3]
4	Nb <sub>2</sub> O <sub>5</sub>	420	2.19	[4]
5	Ni/CdS <sub>8</sub>	420	11.0	[5]
6	AuNC/2D-BiOCl	455-460	4.9	[6]
7	Au/SnS <sub>2</sub> nanosheets	400-500	0.31	[7]

### 3. <sup>1</sup>H NMR spectra of the obtained condensation products

*N*-Benzylidenebenzylamine (**1**): The crude product **1** was purified by chromatography on silica gel (petroleum ether/ethyl acetate, 5: 1). Depurated product **1** was identified by <sup>1</sup>H NMR spectrum (see Figure S2. <sup>1</sup>H NMR (500 MHz, CDCl<sub>3</sub>) δ (ppm): 8.43 (s, 1 H, Ar-CH=N-), 7.83-7.29 (m, 10 H, ArH), 4.86 (s, 2 H, Ar-CH<sub>2</sub>-N-).

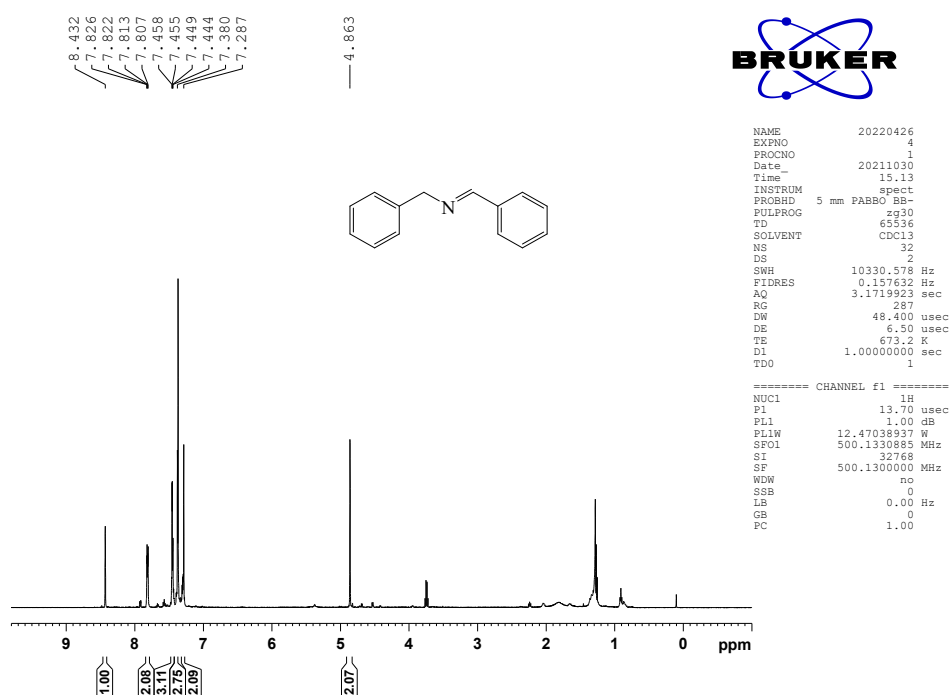


**Figure S2.** <sup>1</sup>H NMR spectrum of product **1**

*N*-(4-Methylbenzylidene)-*p*-methylbenzylamine (**2**): The crude product **2** was purified by chromatography on silica gel (petroleum ether/ethyl acetate, 5: 1). Depurated product **2** was identified by <sup>1</sup>H NMR spectrum (see Figure S3). <sup>1</sup>H NMR (500 MHz, CDCl<sub>3</sub>) δ (ppm): 8.37 (s, 1 H, Ar-CH=N-), 7.70-7.17 (m, 8 H, ArH), 4.80 (s, 2 H, Ar-CH<sub>2</sub>-N=C-), 2.41 (s, 3 H, CH<sub>3</sub>-Ar-), 2.36 (s, 3 H, CH<sub>3</sub>-Ar-).

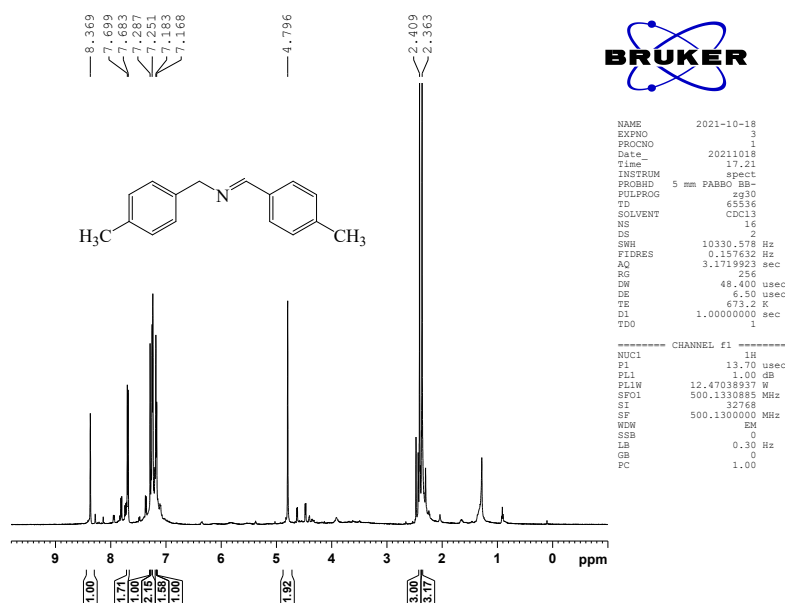
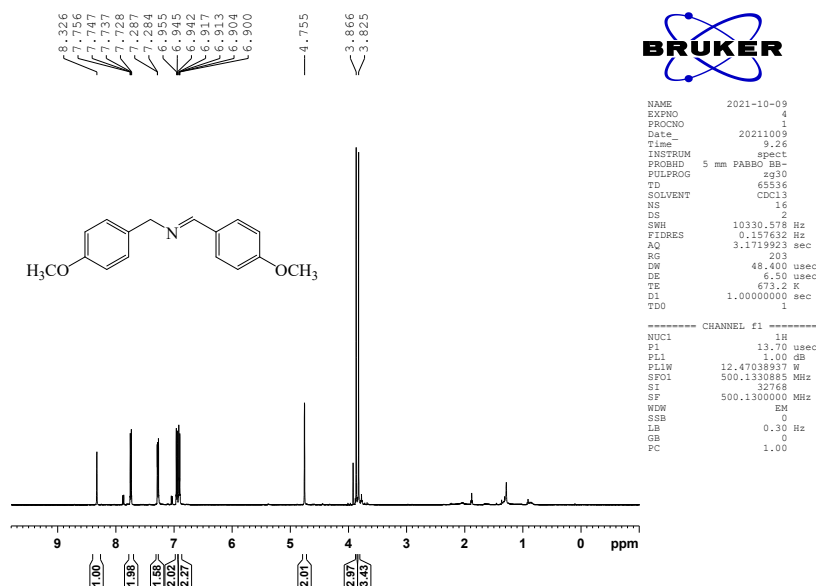
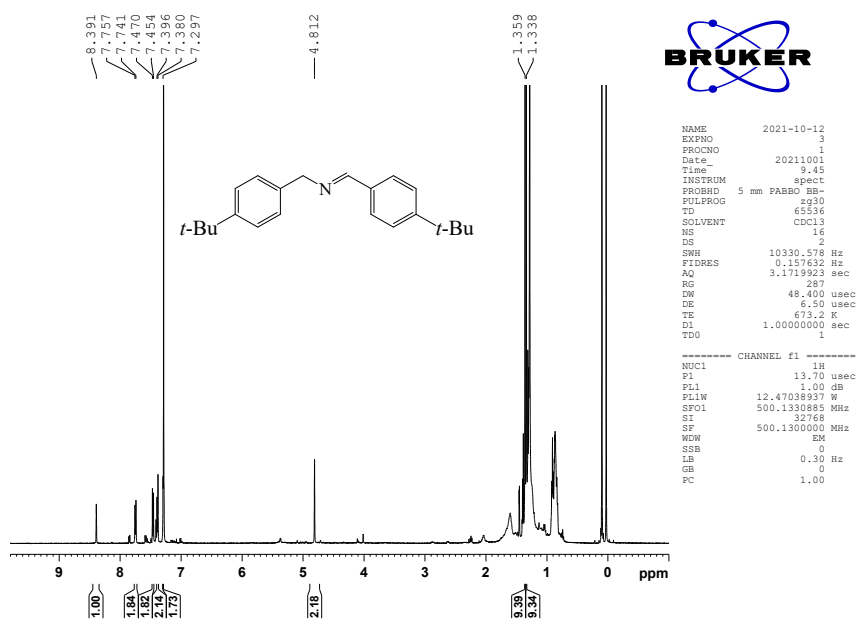


**Figure S3.** <sup>1</sup>H NMR spectrum of product **2**

*N*-(4-Methoxybenzylidene)-*p*-methoxybenzylamine (**3**): The crude product **3** was purified by chromatography on silica gel (petroleum ether/ethyl acetate, 5: 1). Depurated product **3** was identified by <sup>1</sup>H NMR spectrum (see Figure S4). <sup>1</sup>H NMR (500 MHz, CDCl<sub>3</sub>) δ (ppm): 8.33 (s, 1 H, Ar-CH=N-), 7.76-6.90 (m, 8 H, ArH), 4.76 (s, 2 H, Ar-CH<sub>2</sub>-N=C-), 3.87 (s, 3 H, CH<sub>3</sub>-O-Ar), 3.83 (s, 3 H, CH<sub>3</sub>-O-Ar).



*N*-(4-*tert*-Butylbenzylidene)-*p*-*tert*-butylbenzylamine (**4**): The crude product **4** was purified by chromatography on silica gel (petroleum ether/ethyl acetate, 5: 1). Depurated product **4** was identified by  $^1\text{H}$  NMR spectrum (see Figure S5).  $^1\text{H}$  NMR (500 MHz,  $\text{CDCl}_3$ )  $\delta$  (ppm): 8.39 (s, 1 H, Ar-CH=N-), 7.76-7.30 (m, 8 H, ArH), 4.81 (s, 2 H, Ar-CH<sub>2</sub>-N=C-), 1.36 (s, 9 H, (CH<sub>3</sub>)<sub>3</sub>-C-), 1.34 (s, 9 H, (CH<sub>3</sub>)<sub>3</sub>-C-).



*N*-(4-Fluorobenzylidene)-*p*-fluorobenzylamine (**5**): The crude product **5** was purified by chromatography on silica gel (petroleum ether/ethyl acetate, 5: 1). Depurated product **5** was identified by <sup>1</sup>H NMR spectrum (see Figure S6). <sup>1</sup>H NMR (500 MHz, CDCl<sub>3</sub>) δ (ppm): 8.38 (s, 1 H, Ar-CH=N-), 7.81-7.04 (m, 8 H, ArH), 4.79 (s, 2 H, Ar-CH<sub>2</sub>-N=C-).

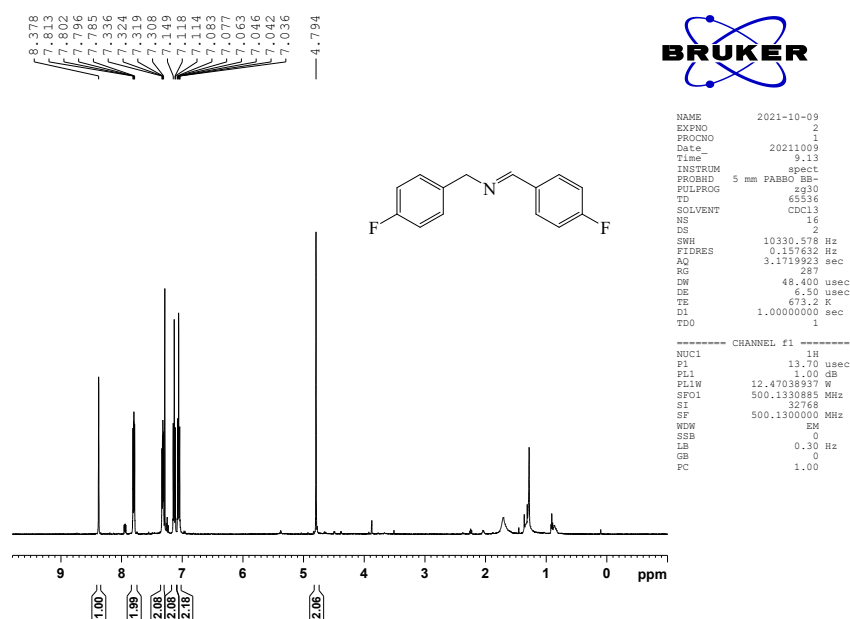


**Figure S6.** <sup>1</sup>H NMR spectrum of product **5**

*N*-(2-Fluorobenzylidene)-*o*-fluorobenzylamine (**6**): The crude product **6** was purified by chromatography on silica gel (petroleum ether/ethyl acetate, 5: 1). Depurated product **6** was identified by <sup>1</sup>H NMR spectrum (see Figure S7). <sup>1</sup>H NMR (500 MHz, CDCl<sub>3</sub>) δ (ppm): 8.76 (s, 1 H, Ar-CH=N-), 8.06-7.09 (m, 8 H, ArH), 4.91 (s, 2 H, Ar-CH<sub>2</sub>-N=C-).



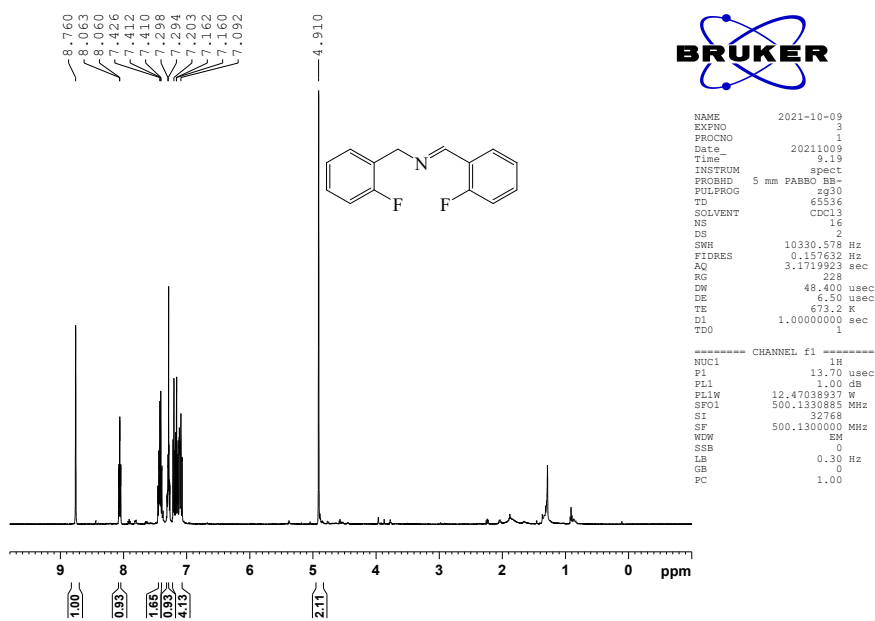


Figure S7.  $^1\text{H}$  NMR spectrum of product 6

*1-(Thiophen-2-yl)-N-(thiophen-2-ylmethyl)methanimine (7)*: The crude product 7 was purified by chromatography on silica gel (petroleum ether/ethyl acetate, 5: 1). Depurated product 7 was identified by  $^1\text{H}$  NMR spectrum (see Figure S8).  $^1\text{H}$  NMR (500 MHz,  $\text{CDCl}_3$ )  $\delta$  (ppm): 8.45 (s, 1 H,  $-\text{CH}=\text{N}-$ ), 7.45-7.01 (m, 6 H,  $-\text{S}-\text{CH}-\text{CH}-\text{C}-$ ), 4.98 (s, 2 H,  $-\text{CH}_2-\text{N}=\text{C}-$ ).

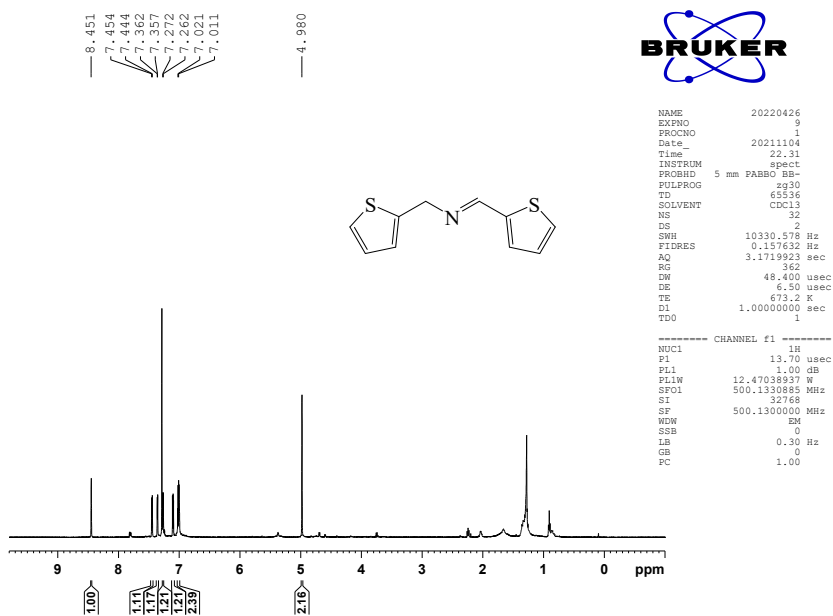


Figure S8.  $^1\text{H}$  NMR spectrum of product 7

## References

- (1) Z. Fang, Z. Deng, X. Wan, Z. Li, X. Ma, S. Hussain, Z. Ye and X. Peng, *Appl. Catal. B Environ.*, 2021, 296, 120329.
- (2) F. Wang, L. Xiao, J. Chen, L. Chen, R. Fang and Y. Li, *ChemSusChem*, 2020, 13, 5711-5721.
- (3) J. Chen, H. Wang, Z. Zhang, L. Han, Y. Zhang, F. Gong, K. Xie, L. Xu, W. Song and S. Wu, *J. Mater. Chem. A*, 2019, 7, 5493-5503.
- (4) S. Furukawa, Y. Ohno, T. Shishido, K. Teramura and T. Tanaka, *J. Phys. Chem. C*, 2013, 117, 442-450.
- (5) W. Yu, D. Zhang, X. Guo, C. Song and Z. Zhao, *Catal. Sci. Technol.*, 2018, 8, 5148-5154.
- (6) H. Chen, L. Peng, Y. Bian, X. Shen, J. Li, H. Yao, S. Zang and Z. Li, *Appl. Catal. B Environ.*, 2021, 284, 119704.
- (7) S. Mondal, L. Sahoo, C. Vinod and U. Gautam, *Appl. Catal. B Environ.*, 2021, 286, 119927.